

## ORIGINAL RESEARCH ARTICLE

# Physicochemical and structural evaluation of natural products as a potential source for viral disease treatment

Fatemeh Mollaamin

Department of Biomedical Engineering, Faculty of Engineering and Architecture, Kastamonu University, Kastamonu 37150, Turkey; [fnollaamin@kastamou.edu.tr](mailto:fnollaamin@kastamou.edu.tr), [smollaamin@gmail.com](mailto:smollaamin@gmail.com)

### ABSTRACT

This research article aims to investigate six selected medicinal plants of *Achillea millefolium* (Yarrow), *Alkanet*, *Rumex patientia* (Patience dock), *Dill*, *Tarragon*, and *Sweet fennel* including some principal chemical compounds of *achillin*, *alkannin*, *cuminaldehyde*, *dillapiole*, *estragole* and *fenchone*. The definitive roles of these medicinal plants in *Omicron* treatment have been investigated through quantum mechanics and molecular mechanic methods. However, given the unprecedented challenges faced should be given a fair amount of consideration for contribution during this pandemic. In this work, it has been investigated the compounds of *achillin*, *alkannin*, *cuminaldehyde*, *dillapiole*, *estragole* and *fenchone* as a probable anti pandemic *Omicron* receptor derived from medicinal plants. Anti-*Omicron* drugs through the hydrogen bonding through physico-chemical properties of medicinal ingredients bound to the database amino acids fragment of Tyr-Met-His as the selective zone of the *Omicron* have been estimated with infrared (IR) and nuclear magnetic resonance (NMR) methods. A comparison of these structures has provided new insights for the design of substrate-based anti-targeting *Omicron*. Finally, five medicinal ingredients of *achillin*, *alkannin*, *cuminaldehyde*, *dillapiole*, and *estragole* bound to TMH have conducted to a Monte Carlo (MC) simulation for evaluating the absorbance of these inhibitor-active site complexes. Here, we used the network pharmacology, metabolite analysis, and molecular simulation to figure out the biochemical basis of the health-raising influence of medicinal plants. This research article peruses the drug ability, metabolites and potential interaction of some medicinal plants with Coronavirus-induced pathogenesis.

**Keywords:** *achillin*; *alkannin*; *cuminaldehyde*; *dillapiole*; *estragole*; *fenchone*; *Omicron* treatment; NMR; IR; medicinal plant

### ARTICLE INFO

Received: 30 June 2023  
Accepted: 23 November 2023  
Available online: 13 March 2024

### COPYRIGHT

Copyright © 2024 by author(s).  
*Applied Chemical Engineering* is published by Arts and Science Press Pte. Ltd. This work is licensed under the Creative Commons Attribution-NonCommercial 4.0 International License (CC BY 4.0).  
<https://creativecommons.org/licenses/by/4.0/>

## 1. Introduction







Recently, antibodies have been almost all produced in human cells, transformed animal cells, and these are platforms that require a lot of equipment, which are very long to set up. Many plant-based antibodies can respond very quickly to the emergence of new variants of coronavirus disease 2019 (COVID-19). The emergence of a new coronavirus, known as a strain of the species severe-acute-respiratory-syndrome-related coronavirus (SARS-CoV-2) has initiated a pandemic of COVID-19. Since its first reported case in Wuhan, China in December 2019, new discovered evidence by both clinicians and researchers globally have helped shed some light on the disease pathogenesis and the nature of the virus itself. The availability of new information subsequently fed policy changes on transmission prevention strategies as well as development of preventative vaccines and therapeutic drug candidates. Enforced physical distancing, hand hygiene, and arguably proper usage of personal protective equipment

including wearing a surgical mask remains the most effective way of controlling the spread of the disease, with most countries which adopted such measures reporting some success in curbing the disease spread<sup>[1-4]</sup>.

In the research of phytomedicine, it is common to observe multiple pharmacological properties from a single plant. It is now well understood that a single plant may contain a wide range of phytochemicals, making ethnopharmacology research both full of possibilities yet challenging. On top of exhibiting direct antiviral effects, medicinal plants with reported anti-inflammatory activities may have pleiotropic roles in COVID-19 management as the elevation of inflammatory markers<sup>[5,6]</sup>.

*Achillea millefolium* or common yarrow is a flowering plant in the family Asteraceae. It is native to temperate regions of the Northern Hemisphere in Asia, Europe, and North America. It has been introduced as a feed for livestock in New Zealand and Australia, where it is a common weed of both wet and dry areas, such as roadsides, meadows, fields and coastal places. *Achillea millefolium* was used as in traditional medicine, possibly due to its astringent effects. Yarrow and its North American varieties were traditionally used by many Native American nations. Native American nations used the plant for healing cuts and abrasions, for relief of ear-aches, and throat infections, and for an eye-wash. Common yarrow was used by Plains indigenous peoples to reduce pain or fever and aid sleep (**Table 1**)<sup>[7,8]</sup>.

**Table 1.** Natural ingredients against Omicron including achillin, alkannin, cuminaldehyde, dillapiole, estragole and fenchone.

| Sources   | Compound      | Applied symptom                     |
|---|---------------|-------------------------------------|
| Dill<br>                                    | Dillapiole    | Anorexia                            |
| Tarragon<br>                               | Estragole     | Anorexia, fever, muscle-joint pain  |
| Sweet fennel<br>                           | Fenchone      | Shortness of breath                 |
| <i>Achillea millefolium</i> (Yarrow)<br>   | Achillin      | Cough, sore throat, nausea-vomiting |
| Alkanet<br>                                | Alkannin      | Diarrhea, skin rash                 |
| <i>Rumex patientia</i> (Patience dock)<br> | Cuminaldehyde | Sore throat, fever, skin rash       |

*Rumex patientia*, known as patience dock<sup>[5]</sup>, garden patience, herb patience, or monk's rhubarb, is a herbaceous perennial flowering plant belonging to the family Polygonaceae. In spring it is often consumed as

a leaf vegetable and as a filling in pies in Southern Europe, especially in Bulgaria, North Macedonia and Serbia. It is also used in Romania in spring broths or sarmale.

*Rumex patientia* or Patience Dock is an uncommon weed of roadsides, farm fields, and waste areas. Some of the distinguishing characteristics of *Rumex patientia* are whether the leaves are crinkly-wavy or relatively flat, the shape of the inner tepals at maturity, size and shape of the grains, whether the grains on all 3 inner tepals are about the same size, sometimes the length of the flower stalk, or where the stalk is jointed, or the vein pattern on the leaves. Patience Dock has weakly crinkly-wavy leaves, tepals up to 8 mm long that are kidney-shaped to nearly round and slightly ragged around the edge, usually a single grain about a quarter as long as the tepal, and the flower stalk has a swollen joint near the base. It has the largest tepals of the Minnesota *Rumex* species, and the (usually) single, small grain makes it unique (**Table 1**)<sup>[9]</sup>.

Dill or *Anethum graveolens* is an annual herb in the celery family Apiaceae. It is the only species in the genus *Anethum*. Dill is grown widely in Eurasia, where its leaves and seeds are used as the herb or spice for flavoring food. Dillapiole, a natural constituent of *Anethum graveolens*, which exhibits potential biological properties. Dillapiole may be used as an analytical reference standard for the quantification of the analyte in French bean *Phaseolus* sp. treated with pesticidal formulation, dill, caraway seeds and pharmaceutical formulations using chromatography techniques (**Table 1**)<sup>[10,11]</sup>.

Tarragon or estragon is a species of perennial herb in the sunflower family. It is widespread in the wild across much of Eurasia and North America, and is cultivated for culinary and medicinal purposes. One subspecies, tarragon is cultivated for use of the leaves as an aromatic culinary herb. In some other subspecies, the characteristic aroma is largely absent (**Table 1**)<sup>[12,13]</sup>.

Sweet fennel is a flowering plant species in the carrot family. It is a hardy, perennial herb with yellow flowers and feathery leaves. It is indigenous to the shores of the Mediterranean but has become widely naturalized in many parts of the world, especially on dry soils near the sea-coast and on riverbanks. It is a highly flavorful herb used in cooking and, along with the similar-tasting anise, is one of the primary ingredients of absinthe (**Table 1**)<sup>[14,15]</sup>.

Several compounds, such as flavonoids, from medicinal plants, have been reported to have antiviral bioactivities<sup>[16–18]</sup>. In the present study, we investigated achillin, alkannin, cuminaldehyde, dillapiole, estragole and fenchone as the probable anti- Omicron receptor derived from natural products (**Table 1**).

Our previous works have been accomplished to collect and depict the values about the major phytochemicals generated by *Artemisia annua*<sup>[19]</sup>, *Asafoetida*<sup>[20]</sup>, several natural products<sup>[21,22]</sup> and to discuss the condition of the chemical properties and biology of the components of this plant against Coronavirus disease infection.

The findings of the present study will provide other researchers with opportunities to identify the right drug to combat Omicron using theoretical methods to estimate the impact of hydrogen bonding in different linkage through seven medicinal plants of achillin, alkannin, cuminaldehyde, dillapiole, estragole and fenchone bound to the active site of Omicron virus.

## 2. Theoretical backgrounds, substances and approaches

The attachment of achillin, alkannin, cuminaldehyde, dillapiole, estragole and fenchone bound to the active site of Omicron protein has been accomplished in this work by forming relatively stable complexes through the hydrogen bonding. Thus, a series of quantum theoretical methods of m062x/cc-pvdz pseudo=CEP for complexes of seven inhibitors for Omicron has been done due to finding the optimized coordination of the best structures of medicinal plant-Tyr160-Met161-His162 drug design model with infrared computations using the Gaussian09 program package<sup>[23]</sup>. It has been indicated that polarization functions into the applied basis set

in the computation always introduce us an important achievement on the modeling and simulation theoretical levels. Normal mode accomplishment is the verdict of harmonic potential wells by analytic methods which maintain the motion of all atoms at the same time in the vibration time scale leading to a natural explanation of molecular vibrations<sup>[23–28]</sup>.

Therefore, the optimized geometry coordination of medicinal ingredients-TMH complexes toward the drug design has been run through the active site of indicated oxygen, nitrogen and hydrogen atoms in the junction of bond and torsion angles (**Table 2**).

**Table 2.** Optimized geometry coordination with m062x/cc-pvdz pseudo=CEP for achillin, cuminaldehyde, dillapiole, and estragole bound to active site of Omicron protein through the drug design method.

| Medicinal ingredients-Omicron active site | Bond angle              | (°)    | Bond distance | (Å)  |
|---|-------------------------|--------|---------------|------|
| <b>Dillapiole</b>                         | N(78)–H(79)–C(13)       | 179.21 | N(78)–H(79)   | 1.03 |
|   |                         |        | H(79)–C(13)   | 1.12 |
|   | N(78)–H(79)–C(13)–O(12) | 55.01  | C(13)–O(12)   | 1.41 |
| <b>Estragole</b>                          | N(71)–H(72)–C(11)       | 179.21 | N(71)–H(72)   | 1.03 |
|   |                         |        | H(72)–C(11)   | 1.12 |
|   | N(71)–H(72)–C(11)–O(10) | 106.92 | C(11)–O(10)   | 1.41 |
| <b>Achillin</b>                           | N(67)–H(68)–O(15)       | 176.18 | N(67)–H(68)   | 1.03 |
|   |                         |        | H(68)–O(15)   | 0.99 |
|   | N(67)–H(68)–O(15)–C(13) | 178.49 | O(15)–C(13)   | 1.41 |
| <b>Cuminaldehyde</b>                      | N(61)–H(62)–O(9)        | 179.19 | N(61)–H(62)   | 1.03 |
|   |                         |        | H(62)–O(9)    | 0.99 |
|   | N(61)–H(62)–O(9)–C(7)   | 31.27  | O(9)–C(7)     | 1.41 |

Therefore, for accomplishing a stable structure of medicinal plant linkage of Omicron active site, geometry optimization plus the NMR estimation, the frequency and intensity of the vibrational modes were calculated with the quantum mechanical method, and the principal vibrational modes were analyzed<sup>[29,30]</sup>.

The theoretical calculations were done at various levels of theory to gain the more accurate equilibrium geometrical results and IR spectral data for each of the identified compounds. It is supposed that an additional diffuse and polarization functions into the basis set applied in the computation conduct us to the magnificent progress on the results of theoretical methods.

The simulation indicates the approaches which produce a common template of a model at a special temperature by computing all physicochemical properties among the partition function<sup>[31–33]</sup>.

Each part of the systems including medicinal ingredients-TMH has been optimized using ab-initio via density functional theory including ECP calculations with pseudo=CEP basis sets. In addition, those systems have been evaluated via quantum mechanics/molecular mechanics (QM/MM) approach through an our Own N-layer Integrated molecular Orbital molecular Mechanics (ONIOM) method. In our study, differences of force fields are debated through comparing density and energies with Optimized Potentials for Liquid Simulations (OPLS) and Assisted Model Building with Energy Refinement (AMBER) via MC simulation. In addition, a Hyperchem professional release 7.01 program has been applied for some additional keywords such as PM3MM, PM6 and pseudo=CEP<sup>[34,35]</sup>.

Moreover, MC simulation has been accomplished on the anti-Omicron drugs This method is a class of computational algorithms that is based on repeated random sampling to estimate the results which is often

applied in simulating physical and mathematical systems.

Computation of random or pseudo-random numbers causes the accuracy of calculation especially for unfeasible or impossible to compute an exact result with a deterministic algorithm<sup>[36]</sup>. It doesn't always need random numbers to use deterministic, pseudo-random sequences, making it easy to test and re-run simulations<sup>[37]</sup>. The new configuration is accepted if the energy decreases and with a probability of  $e^{-\Delta E/kT}$  if the energy increases. This Metropolis procedure ensures that the configurations in the ensemble obey a Boltzmann distribution, and the possibility of accepting higher energy configurations allows MC methods to climb uphill and escape from a local minimum<sup>[37]</sup>. MC simulations require only the ability to evaluate the energy of the system, which may be advantageous if calculating the first derivative is difficult or time-consuming. Furthermore, since only a single particle is moved in each step, only the energy changes associated with this move must be calculated, not the total energy for the whole system. A disadvantage of MC methods is the lack of the time dimension and atomic velocities, and they are therefore not suitable for studying time-dependent phenomena or properties depending on momentum<sup>[37]</sup>.

### 3. Results and discussion

#### 3.1. NMR analysis

NMR shifts on the database of amino acids in beta sheet conformation of Tyr160-Met161-His162 and the four main ingredients of medicinal plants including achillin, alkannin, cuminaldehyde, dillapiole, estragole and fenchone have been estimated to unravel the indicated atoms of H, N, O in the active sites of these anti-virus drugs through the formation of hydrogen bonding by indicating the attack zone of TMH (**Figure 1a-f**).

Achillin, alkannin, cuminaldehyde, dillapiole, estragole and fenchone have approximately shown the identical behavior (about 30–200 ppm) for various atoms in the interaction site of these compounds with Tyr160-Met161-His162 through the NMR calculations (**Figure 1**). The sharpest peak of NMR spectrum has been almost observed in 30 ppm for all principal ingredients of herbal medicine. The weakest peaks of NMR spectrum have approximately appeared between 50–200 ppm (**Figure 1**).

The NMR measurements demonstrate the active sites of main ingredients of medicinal species for linking to the Tyr160-Met161-His162 (TMH) in forming the anti-virus drugs while each active atom of oxygen and nitrogen as the electronegative atoms for attaching to the hydrogen denotes the maximal shift in all levels in the NMR spectra (**Figure 1a-f**).

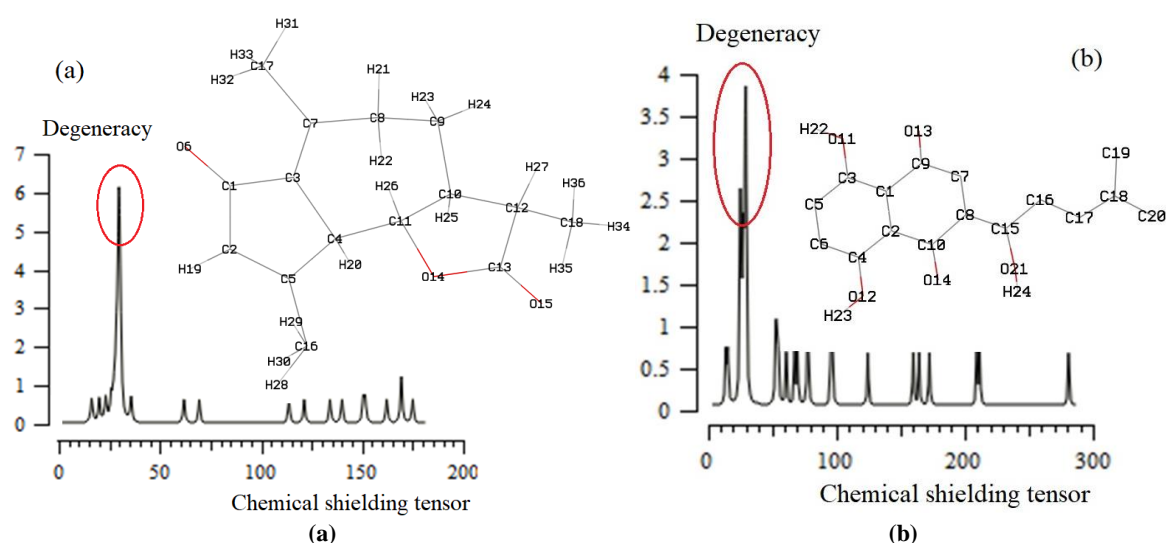


**Figure 1.** (Continued).

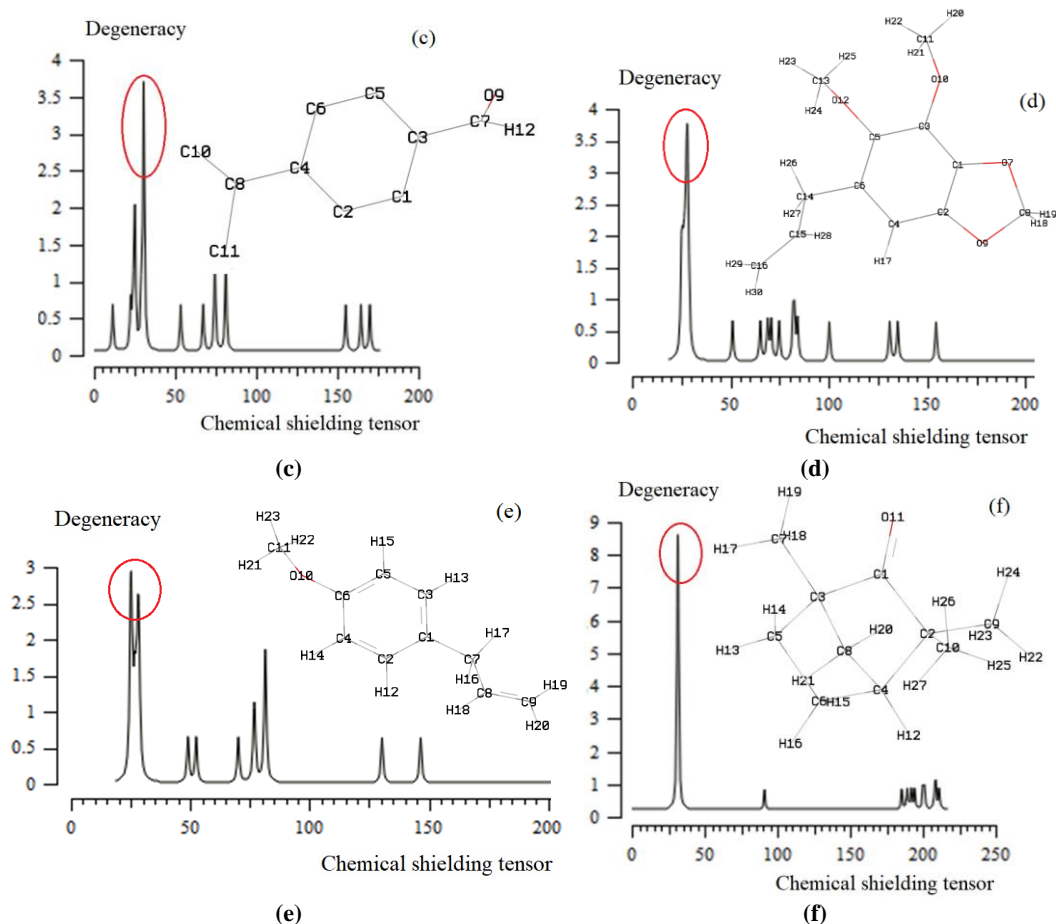


**Figure 1.** The graphs of NMR spectra for (a) achillin; (b) alkannin; (c) cuminaldehyde; (d) dillapiole; (e) estragole; and (f) fenchone bound to TMH Omicron active site through the drug design method by indicating the active zone of TMH in the drug design process.

### 3.2. IR spectra analysis and thermodynamic properties

The technique of IR for main ingredients of medicinal plants including achillin, alkannin, cuminaldehyde, dillapiole, estragole and fenchone have been computed for stabilizing the junction of Tyr160-Met161-His162 as the anti-Omicron through the drug design method using IR spectroscopy using Gaussian09 to obtain the best amounts for geometrical coordination and thermochemical parameters (**Figure 2a–f**). The most fluctuation of frequency of IR spectra for alendronic acid, ibandronic acid, neridronic acid, and pamidronic acid has been approximately seen between 0–3000  $\text{cm}^{-1}$ . The sharpest peak of IR spectrum has been approximately observed in 2000  $\text{cm}^{-1}$  for all principal ingredients of herbal medicine.

The strongest peaks of IR graph for principal ingredients of herbal medicine have been observed in 1850  $\text{cm}^{-1}$  for achillin (**Figure 2a**), in 2000  $\text{cm}^{-1}$  for alkannin (**Figure 2b**), in 1950  $\text{cm}^{-1}$  for cuminaldehyde (**Figure 2c**), in 2050  $\text{cm}^{-1}$  for dillapiole (**Figure 2d**), in 1850  $\text{cm}^{-1}$  for estragole  $\text{cm}^{-1}$  (**Figure 2e**), and in 2125  $\text{cm}^{-1}$  for fenchone (**Figure 2f**). In achillin, cuminaldehyde, dillapiole, and estragole jointed to the database of amino acids in beta sheet conformation, Tyr160-Met161-His162, as the active site of Omicron protein in the process of drug design, the frequency and intensity of various infrared normal modes of medicinal ingredients-TMH complexes have been found to be significantly different through the stability of H-bonding formed between active site of Omicron variant B.1.1.529 and medicinal ingredients which founds the anti-Omicron Variant (**Table 3** and **Figure 3**).

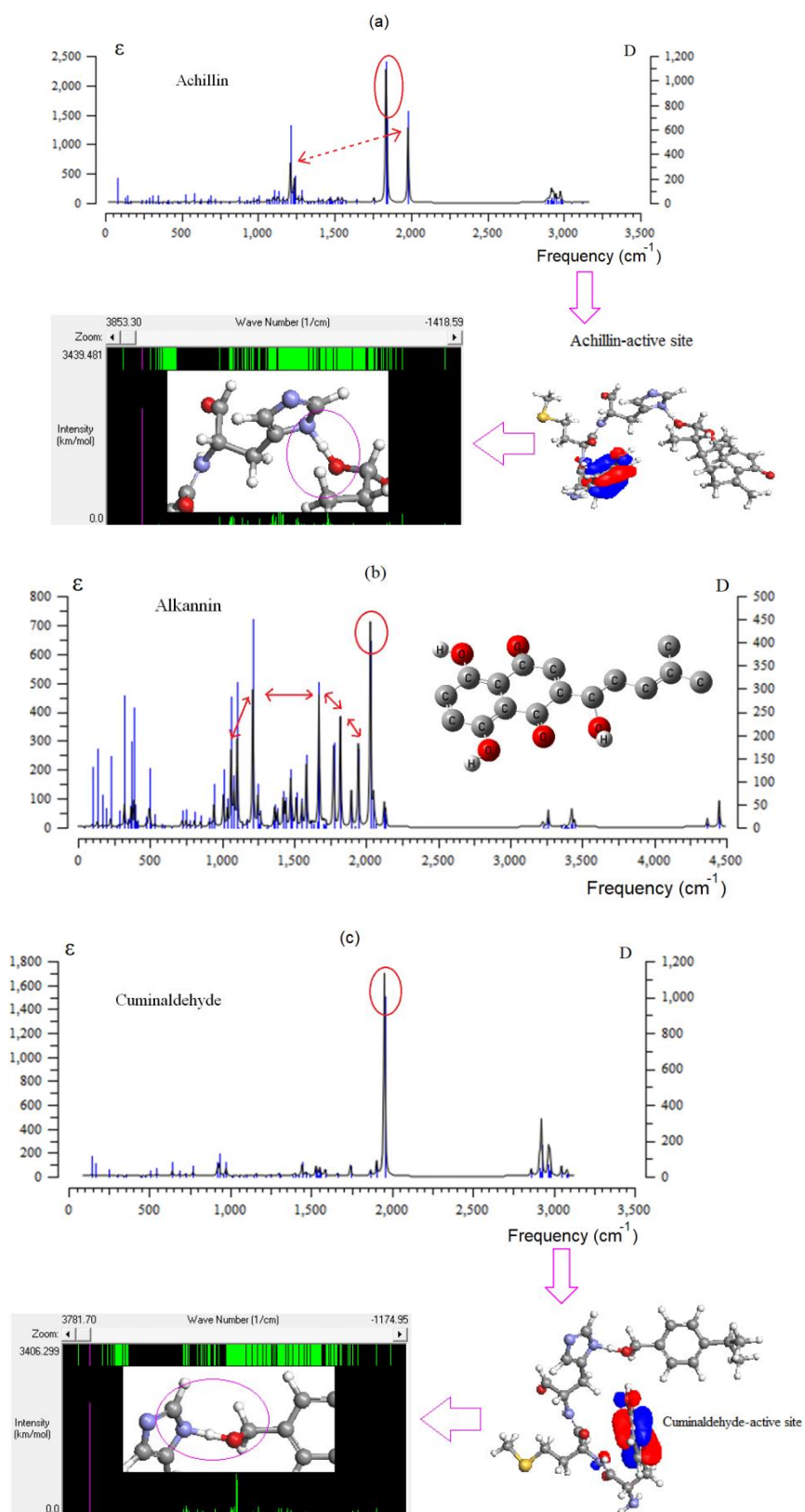
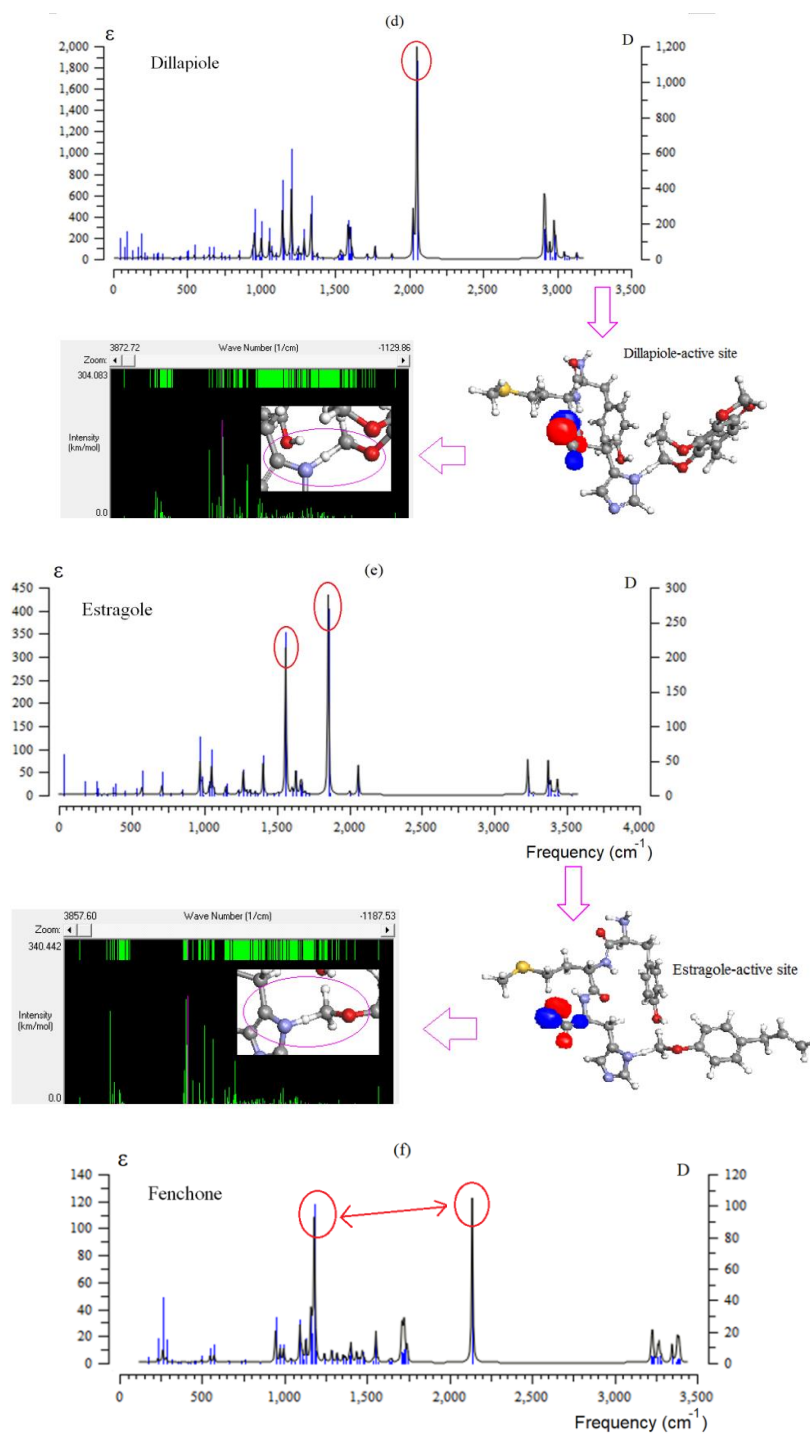


Figure 2. (Continued).



**Figure 2.** IR spectrum of (a) achillin; (b) alkannin; (c) cuminaldehyde; (d) dillapiole; (e) estragole; and (f) fenchone bound to TMH through the drug design method calculated by m062x/cc-pvdz pseudo = CEP.

**Table 3.** Achillin, cuminaldehyde, dillapiole, and estragole as anti-Omicron drugs in different normal modes of infrared spectra.

| Inhibitor     | Intensity (km/mol) | Frequency (1/cm) | Normal mode |
|---------------|--------------------|------------------|-------------|
| Achillin      | 2292.987           | 3336.01          | 275         |
| Cuminaldehyde | 2270.866           | 3395.38          | 236         |
| Dillapiole    | 202.722            | 1998.66          | 205         |
| Estragole     | 226.961            | 1971.26          | 185         |



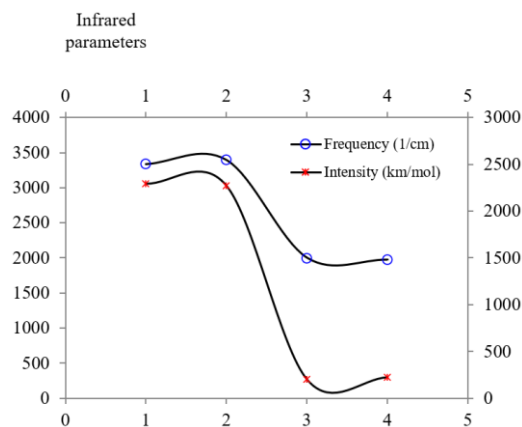


**Figure 3.** IR spectrum for medicinal plants of achillin, cuminaldehyde, dillapiole, estragole anti-Omicron drugs in normal mode = 59.

The frequency and intensity TMH-junction were found to be significantly different with each medicinal ingredient treatment including achillin, cuminaldehyde, dillapiole, estragole and fenchone. It has been seen that the frequency and intensity for achillin, cuminaldehyde are higher than dillapiole and estragole (**Figure 3**).

Then, thermodynamic properties have determined the stable anti-Omicron variant complexes of main ingredients of medicinal species-TMH through the H-bonding formation using the drug design method (**Table 4**).

**Table 4.** Thermodynamic factors of achillin, alkannin, cuminaldehyde, dillapiole and estragole bound to Omicron active site protein.

| Plant component-active site | $E_{\text{electronic}} \times 10^{-4}$<br>(kcal/mol) | $E_{\text{core-core}} \times 10^{-4}$<br>(kcal/mol) | $\Delta G \times 10^{-4}$<br>(kcal/mol) | $\Delta S$<br>(kcal/K.mol) |
|-----------------------------|--|---|---|----------------------------|
| <b>Achillin</b>             | -214.36  | 196.14  | -18.21                                  | 607.28                     |
| <b>Alkannin</b>             | -232.37  | 212.67  | -19.69                                  | 656.56                     |
| <b>Cuminaldehyde</b>        | -165.89  | 150.60  | -15.28                                  | 509.72                     |
| <b>Dillapiole</b>           | -198.48  | 180.62  | -17.85                                  | 595.29                     |
| <b>Estragole</b>            | -160.68  | 145.47  | -15.21                                  | 507.37                     |

Furthermore, the difference of  $\Delta H_F$  among achillin, alkannin, cuminaldehyde, dillapiole, and estragole bound to Omicron has been discussed the H-bonding due to the database of amino acids in beta sheet conformation; Tyr160-Met161-His162 as the active site of the Omicron molecule (**Table 5** and **Figure 4**).

**Table 5.** The Heat of formation,  $\Delta H_F$  (kcal/mol), among achillin, alkannin, cuminaldehyde, dillapiole, and estragole bonded to Omicron active site (TMH) complexes at 300 K.

| $\Delta H_{\text{TMH}} \times 10^{-4}$ 25.8242 (kcal/mol) |   |   |
|---|---|---|
| $\Delta H_{\text{Achillin}}$                              | $\Delta H_{\text{(Achillin-active site)}}$      | $\Delta H_F \times 10^{-4} = \Delta H_{\text{(Achillin-active site)}} - (\Delta H_{\text{Achillin}} + \Delta H_{\text{active site}})$           |
| -76.24  | 9.54  | -25.81  |
| $\Delta H_{\text{Alkannin}}$                              | $\Delta H_{\text{(Alkannin-active site)}}$      | $\Delta H_F \times 10^{-4} = \Delta H_{\text{(Alkannin-active site)}} - (\Delta H_{\text{Alkannin}} + \Delta H_{\text{active site}})$           |
| -80.84  | -1.40   | -25.81  |
| $\Delta H_{\text{Cuminaldehyde}}$                         | $\Delta H_{\text{(Cuminaldehyde-active site)}}$ | $\Delta H_F \times 10^{-4} = \Delta H_{\text{(Cuminaldehyde-active site)}} - (\Delta H_{\text{Cuminaldehyde}} + \Delta H_{\text{active site}})$ |
| -3.67   | 67.84   | -25.81  |
| $\Delta H_{\text{Dillapiole}}$                            | $\Delta H_{\text{(Dillapiole-active site)}}$    | $\Delta H_F \times 10^{-4} = \Delta H_{\text{(Dillapiole-active site)}} - (\Delta H_{\text{Dillapiole}} + \Delta H_{\text{active site}})$       |
| -31.34  | 33.10   | -25.81  |
| $\Delta H_{\text{Estragole}}$                             | $\Delta H_{\text{(Estragole-active site)}}$     | $\Delta H_F \times 10^{-4} = \Delta H_{\text{(Estragole-active site)}} - (\Delta H_{\text{Estragole}} + \Delta H_{\text{active site}})$         |
| 101.56  | 14.90   | -25.83  |

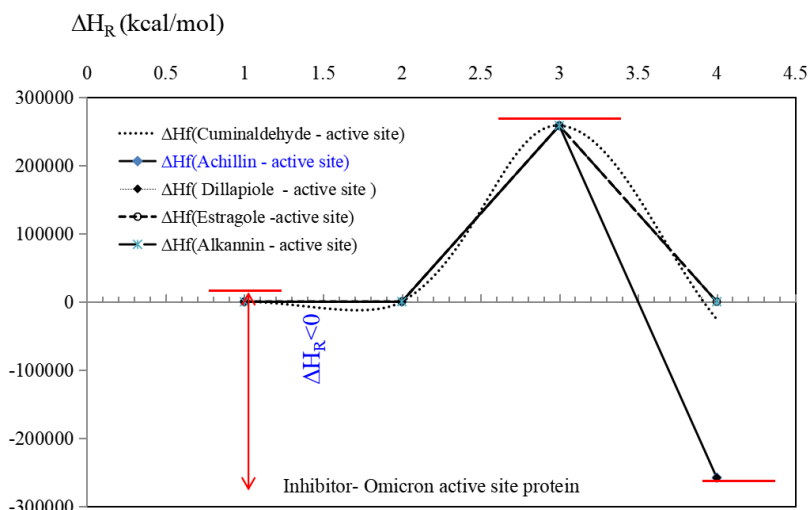


**Figure 4.** The changes of  $\Delta H_R$  among achillin, alkannin, cuminaldehyde, dillapiole, and estragole bound to Omicron active site protein.

### 3.3. Charge distribution

In the next step, the atomic charge of indicated atoms of oxygen junction of achillin, alkannin, cuminaldehyde, dillapiole, and estragole with Tyr160-Met161-His162 have been evaluated in the zone of H-bonding formation (**Table 6**).

**Table 6.** The values of atomic charge for labeled oxygen atoms in the attachment of achillin, alkannin, cuminaldehyde, dillapiole, and estragole with Tyr160-Met161-His162.

| Achillin | Charge | Alkannin | Charge | Cuminaldehyde | Charge | Dillapiole | Charge | Estragole | Charge |
|----------|--------|----------|--------|---------------|--------|------------|--------|-----------|--------|
| N(19)    | -0.04  | N(24)    | -0.04  | N(13)         | -0.04  | N(30)      | -0.04  | N(23)     | -0.04  |
| N(40)    | -0.05  | N(45)    | -0.05  | N(34)         | -0.05  | N(51)      | -0.05  | N(44)     | -0.05  |
| N(57)    | -0.03  | N(62)    | -0.03  | N(51)         | -0.03  | N(68)      | -0.03  | N(61)     | -0.03  |
| N(67)    | 0.10   | N(72)    | 0.00   | N(61)         | 0.05   | N(78)      | 0.38   | N(71)     | 0.24   |
| N(73)    | -0.11  | N(78)    | -0.09  | N(67)         | -0.12  | N(84)      | -0.04  | N(77)     | -0.05  |
| O(14)    | -0.25  | O(11)    | -0.45  | O(9)          | -0.45  | O(9)       | -0.15  | O(10)     | -0.19  |
| O(15)    | -0.42  | O(12)    | -0.19  | O(18)         | -0.40  | O(10)      | -0.17  | O(28)     | -0.40  |
| O(24)    | -0.40  | O(14)    | -0.31  | O(32)         | -0.24  | O(12)      | -0.17  | O(42)     | -0.23  |
| O(38)    | -0.23  | O(21)    | -0.34  | O(39)         | -0.38  | O(490)     | -0.21  | O(49)     | -0.38  |
| O(45)    | -0.38  | O(29)    | -0.40  | O(56)         | -0.31  | O(56)      | -0.38  | O(66)     | -0.32  |
| O(62)    | -0.30  | O(43)    | -0.26  | -             | -      | O(73)      | -0.32  | -         | -      |
| -        | -      | O(50)    | -0.38  | -             | -      | -          | -      | -         | -      |
| -        | -      | O(67)    | -0.29  | -             | -      | -          | -      | -         | -      |

Then, in **Figure 5**, it has been plotted the changes of atomic charge for labeled oxygen atoms through optimized achillin, alkannin, cuminaldehyde, dillapiole, and estragole with Tyr160-Met161-His162 complexes due to formation of H-bonding; so, the results of **Table 6** in a polar zone have declared the stability of Omicron drugs which have been accomplished considering the oxygen as the electronegative atoms in formation the H-bonding through using the drug design method which has suggested the modeling of anti-Omicron.

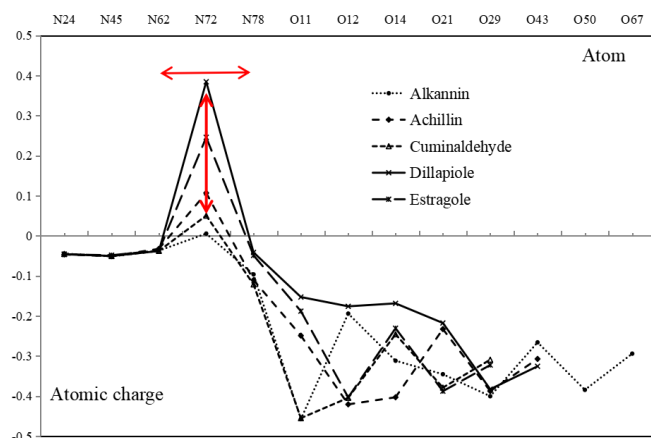


**Figure 5.** Comparison of atomic charge versus labeled of oxygen atoms in the junction of active sites of achillin, alkannin, cuminaldehyde, dillapiole, and estragole with Tyr160-Met161-His162.

Thus, the perspective of **Figure 5** has proposed the reason for existing observed various results of the atomic charge on medicinal plant-Omicron complexes as the anti-Omicron drugs which are principally related to the position of active sites of indicated oxygen, nitrogen and hydrogen atoms in the junction of bond angles. In fact, the spin density and partial charges have been obtained by fitting the electrostatic potential to fix the charge of oxygen and nitrogen with high electronegativity in junction of electrophilic group of hydrogen in the structures of medicinal plant-Omicron as the anti-virus drugs which conduct us toward the industry of drug design.

### 3.4. MC simulation

Then, achillin, alkannin, cuminaldehyde, dillapiole, and estragole bound to TMH have directed to a MC simulation by potential energy in 300 K via time scale (0–100) with max delta and time steps of 0.05 Å, 1, respectively (**Figure 6**). Optimal values are close to 0.5. Differencing the step size can have a large influence on the acceptance ratio. The MC options dialog box lets us arrange the MC simulation parameters with 100 steps.

Study of the solution state has invoked much interest among investigators and a lot has been done in the study of solute-solvent interactions. Water is the main solvent environment for a majority of biomolecules. It has been estimated the potential of achillin, alkannin, cuminaldehyde, dillapiole, and estragole with a simulated model of solute-solvent in a periodic box with maximum number of water molecules, minimum distance between solvent and solute molecules using program package HyperChem 8<sup>[38–44]</sup>. It has been shown the potential energy graph of achillin, alkannin, cuminaldehyde, dillapiole, and estragole in solvent via time scale (0–100) in 300 K using MC method (max delta = 0.05 Å, time steps = 1).

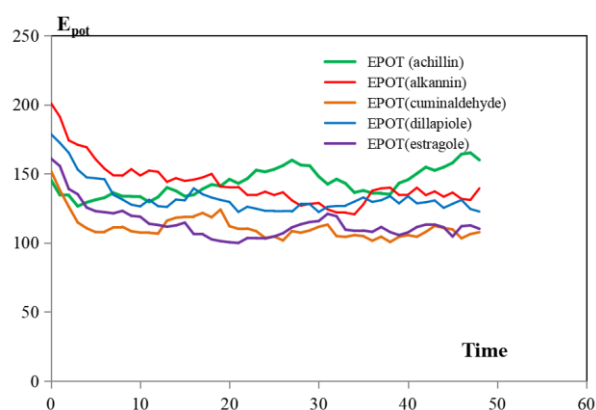


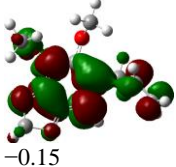
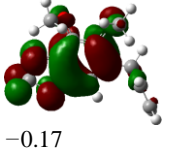
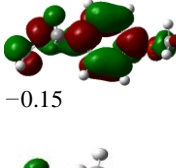
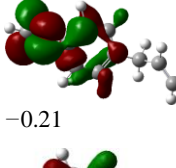
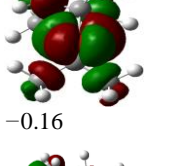
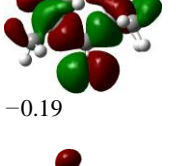
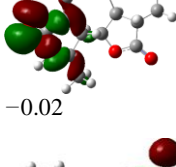
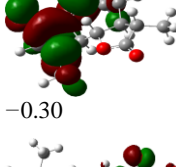
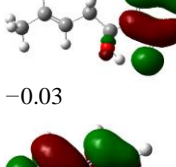
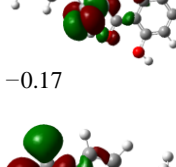
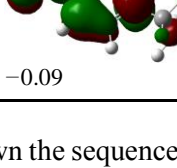
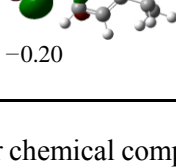
**Figure 6.** MC simulation of achillin, alkannin, cuminaldehyde, dillapiole, and estragole bound to TMH as the anti-Omicron drugs.

The results of the above observations strongly suggest that the different data observed in the achillin, alkannin, cuminaldehyde, dillapiole, and estragole in the solvent is predominantly due to basis set functions, induced by a change in polarity of the environment. It is clear that an increase in the dielectric constants increases the stability of these anti-Omicron drugs.

### 3.5. HOMO & LUMO: Frontier orbitals

The highest occupied molecular orbital energy (HOMO) and the lowest unoccupied molecular orbital energy (LUMO) have been calculated for some effective ingredients of achillin, alkannin, cuminaldehyde, dillapiole, estragole and fenchone (**Table 7**). The HOMO, LUMO and band energy gap (eV) indicated the pictorial explanation of the frontier molecular orbital's and their respective positive and negative zones which are an important factor for identifying the molecular characteristics of achillin, alkannin, cuminaldehyde, dillapiole, estragole and Fenchone in of six selected medicinal plants of *Achillea millefolium* (Yarrow), Alkanet, Rumex patientia (Patience dock), Dill, Tarragon, and Sweet fennel.

**Table 7.** The HOMO (a.u.), LUMO (a.u.), and band energy gap (eV) of dillapiole, estragole, Fenchone, achillin, alkannin, and cuminaldehyde.

| Molecule      | $E_{LUMO}$  | $E_{HOMO}$   | $\Delta E$ |
|---------------|---|--|------------|
| Dillapiole    |  -0.15  |  -0.17  | 0.38       |
| Estragole     |  -0.15 |  -0.21 | 1.68       |
| Fenchone      |  -0.16 |  -0.19 | 0.82       |
| Achillin      |  -0.02 |  -0.30 | 7.49       |
| Alkannin      |  -0.03 |  -0.17 | 4.04       |
| Cuminaldehyde |  -0.09 |  -0.20 | 3.23       |

**Table 7** has shown the sequence of band energy gap for chemical compounds of natural drugs as:  $\Delta E_{achillin} > \Delta E_{alkannin} > \Delta E_{cuminaldehyde} > \Delta E_{estragole} > \Delta E_{fenchone} > \Delta E_{dillapiole}$  with the relation coefficient of  $R^2 = 0.9374$ . While the band energy gap ( $\Delta E$ ) decreases, the stability of the compound increases. Therefore, the fenchone is

predicted to be more sensitive than other ingredients.

In other words, the HOMO shows the capability for giving an electron while the LUMO as an electron acceptor exhibits the capability for achieving an electron. Therefore, the energy gap ( $\Delta E = E_{\text{LUMO}} - E_{\text{HOMO}}$ ) indicates the energy difference between frontier HOMO and LUMO orbital introducing the stability for the structure and unravels the chemical activity of the molecule. In this work, energy gap establishes how achillin, alkannin, cuminaldehyde, dillapiole, estragole and fenchone as an efficient anti pandemic Omicron receptor derived from medicinal plants. Besides, frontier molecular orbitals run an important function in the optical and electrical properties like in UV-Vis spectra<sup>[45-49]</sup>.

The results in this article have manifested that medicinal plants and phytochemicals can have a considerable function due to their substantial antiviral activity against Omicron, SARS-CoV-2 and other coronaviruses. Achillin, alkannin, cuminaldehyde, dillapiole, estragole and Fenchone extracted from *Achillea millefolium* (Yarrow), *Alkanet*, *Rumex patientia* (Patience dock), Dill, Tarragon, and Sweet fennel, respectively, were identified through in-silico molecular modeling by using DFT screening. Identified natural phytochemicals revealed to be potential in exhibiting antiviral activities by disrupting the viral life cycle including viral entrance, replication, assembly, and discharge, as well as virus specific host targets. Thus, this prompts increasing of pharmaceutical industry focused on phytochemical extracts from medicinal plants, and aromatic herbs in the hopes of discovering lead compounds, with purposeful to antiviral medications.

Here, we used the network pharmacology, metabolite analysis, and molecular simulation to comprehend the biochemical basis of the health-boosting impact of medicinal plants. The present study investigates the drug ability, metabolites and potential interaction of the title tea with genes associated with Omicron-induced pathogenesis.

Altogether, the evidence presented in this work supports the notion that medicinal plants have promising therapeutic potential, especially in the case of herb products against viral infections.

## 4. Conclusion

The results in this article have remarked that medicinal plants due to potential active phytochemicals might grow a further effective species in the remedy of Omicron variant. Some physical and physicochemical attributes from optimized structure of achillin, alkannin, cuminaldehyde, dillapiole, estragole and fenchone joined to the database amino acids fragment of Tyr160-Met161-His162 as the selective zone of the Omicron have been distinguished. Then, the fluctuation in the NMR chemical shift has been estimated which might have been affected by the atomic configuration of the anti-virus.

The stability of H-bonding between several medicinal ingredients of achillin, alkannin, cuminaldehyde, dillapiole, estragole, fenchone and Omicron through the formation anti-Omicron through two probabilities of  $\text{N} \cdots \text{H}$  and  $\text{O} \cdots \text{H}$  with different atomic charges have been investigated using IR methods. So, the thermodynamic properties of Gibbs free energy, enthalpy of formation, electronic energy, core-core interaction have approved the stability of anti-Omicron due to H-bonding formation using the drug design method. The simulations of medicinal ingredients-Omicron show that the stabilization energy has been affected by the MC force field and different temperature and the best results have been gained for potential energy vs. temperature at MC force field and by increasing of temperature, our calculations have demonstrated that such extrapolation schemes significantly overestimate the medicinal ingredients-Omicron by active site of molecule (N and O linkage) which are the most active point at indicated structure.

Moreover, the lowering of the energy gap ( $\Delta E = E_{\text{LUMO}} - E_{\text{HOMO}}$ ) has illustrated the charge transfer interactions taking place within achillin, alkannin, cuminaldehyde, dillapiole, estragole, and fenchone. The atomic charges have donated the proper perception of the molecular theory and the energies of fundamental

molecular orbitals.

## Acknowledgments

In successfully completing this paper and its research, the author is grateful to Kastamonu University.

## Conflict of interest

The author declares no conflict of interest.

## References

1. Sardar T, Nadim SS, Rana S, et al. Assessment of lockdown effect in some states and overall India: A predictive mathematical study on COVID-19 outbreak. *Chaos, Solitons & Fractals*. 2020, 139: 110078. doi: 10.1016/j.chaos.2020.110078
2. Chu DK, Akl EA, Duda S, et al. Physical distancing, face masks, and eye protection to prevent person-to-person transmission of SARS-CoV-2 and COVID-19: a systematic review and meta-analysis. *The Lancet*. 2020, 395(10242): 1973–1987. doi: 10.1016/s0140-6736(20)31142-9
3. Bonaccorsi G, Pierri F, Cinelli M, et al. Economic and social consequences of human mobility restrictions under COVID-19. *Proceedings of the National Academy of Sciences*. 2020, 117(27): 15530–15535. doi: 10.1073/pnas.2007658117
4. Zadeh MAA, Lari H, Kharghanian L, et al. Density Functional Theory Study and Anti-Cancer Properties of Shyshaq Plant: In View Point of Nano Biotechnology. *Journal of Computational and Theoretical Nanoscience*. 2015, 12(11): 4358–4367. doi: 10.1166/jctn.2015.4366
5. Süntar I. Importance of ethnopharmacological studies in drug discovery: role of medicinal plants. *Phytochemistry Reviews*. 2019, 19(5): 1199–1209. doi: 10.1007/s11101-019-09629-9
6. Zeng F, Huang Y, Guo Y, et al. Association of inflammatory markers with the severity of COVID-19: A meta-analysis. *International Journal of Infectious Diseases*. 2020, 96: 467–474. doi: 10.1016/j.ijid.2020.05.055
7. Maiz-Tome L. *Achillea millefolium*. IUCN Red List of Threatened Species. 2016: e.T202909A78457012. doi: 10.2305/IUCN.UK.2016-1.RLTS.T202909A78457012.en
8. Faran M, Tcherni A. *Medicinal herbs in Modern Medicine (Hebrew)*. Jerusalem: Akademon (Hebrew University of Jerusalem). 1997, 1: 242.
9. Crawford M. *How to grow Perennial Vegetables*. 2012.
10. Nam HH, Nan L, Choo BK. Anti-Inflammation and Protective Effects of *Anethum graveolens* L. (Dill Seeds) on Esophageal Mucosa Damages in Reflux Esophagitis-Induced Rats. *Foods* 2021, 10: 2500. doi:10.3390/foods10102500.
11. Hall D. Eastern Black Swallowtail: *Papilio polyxenes asterius* (Stoll) (Insecta: Lepidoptera: Papilionidae). *edis.ifas.ufl.edu*. 2017.
12. Shultz LM. *Artemisia dracunculus*. In *Flora of North America Editorial Committee (ed.)*. *Flora of North America North of Mexico (FNA)*. New York and Oxford—via eFloras.org, Missouri Botanical Garden, St. Louis, MO & Harvard University Herbaria, Cambridge, MA. 2006.
13. Zeller A, Rychlik M. Impact of estragole and other odorants on the flavour of anise and tarragon. *Flavour and Fragrance Journal*. 2006, 22(2): 105–113. doi: 10.1002/ffj.1765
14. Ribeiro-Santos R, Andrade M, Sanches-Silva A, et al. Essential Oils for Food Application: Natural Substances with Established Biological Activities. *Food and Bioprocess Technology*. 2017, 11(1): 43–71. doi: 10.1007/s11947-017-1948-6
15. Badgujar SB, Patel VV, Bandivdekar AH. *Foeniculum vulgare* Mill: A Review of Its Botany, Phytochemistry, Pharmacology, Contemporary Application, and Toxicology. *BioMed Research International*. 2014, 2014: 1–32. doi: 10.1155/2014/842674
16. Zakaryan H, Arabyan E, Oo A, et al. Flavonoids: promising natural compounds against viral infections. *Archives of Virology*. 2017, 162(9): 2539–2551. doi: 10.1007/s00705-017-3417-y
17. Seema TM, Thyagarajan SP. Pa-9: A flavonoid extracted from *Plectranthus amboinicus* inhibits HIV-1 protease. *Int. J. Pharmacogn. Phytochem. Res*. 2016, 8(6), 1020–1024.
18. Jo S, Kim S, Shin DH, et al. Inhibition of SARS-CoV 3CL protease by flavonoids. *Journal of Enzyme Inhibition and Medicinal Chemistry*. 2019, 35(1): 145–151. doi: 10.1080/14756366.2019.1690480
19. Mollaamin F, Monajjemi M, Mohammadi S. Physicochemical Characterization of Antiviral Phytochemicals of *Artemisia annua* Plant as Therapeutic Potential against Coronavirus Disease: In Silico–Drug Delivery by Density Functional Theory Benchmark. *J. Biol. Regul. Homeost. Agents*. 2023; 37(7): 3629–3639. doi: 10.23812/j.biol.regul.homeost.agents.20233707.358
20. Mollaamin F, Shahriari S, Monajjemi M. Treating omicron BA. 4 & BA. 5 via herbal antioxidant asafoetida: A dft study of carbon nanocarrier in drug delivery. *Journal of the Chilean Chemical Society*. 2023; 68: 5781–5786.

doi:10.4067/S0717-97072023000105781

21. Zheng Q, Yan C, Lv N, et al. Natural Products for Omicron BA.1, BA.1.1 and BA.2 Therapy: Application of Medicinal Plants for Drug Delivery: A DFT & QM/MM Simulation. *J. Biol. Regul. Homeost. Agents. J. Biol. Regul. Homeost. Agents.* 2023; 37(6): 3403–3416. doi: 10.23812/j.biol.regul.homeost.agents.20233706.337
22. Mollaamin F, Monajjemi M. Thermodynamic research on the inhibitors of coronavirus through drug delivery method. *Journal of the Chilean Chemical Society.* 2021, 66(2): 5195–5205. doi: 10.4067/s0717-97072021000205195
23. Frisch MJ, Trucks GW, Schlegel HB, et al. Gaussian 09, Revision B.01. 2010. Gaussian Inc., Wallingford.
24. Khalili Hadad B, Mollaamin F, Monajjemi M. Biophysical chemistry of macrocycles for drug delivery: a theoretical study. *Russian Chemical Bulletin.* 2011, 60(2): 238–241. doi: 10.1007/s11172-011-0039-5
25. Roy TK, Kopysov V, Pereverzev A, et al. Intrinsic structure of pentapeptide Leu-enkephalin: geometry optimization and validation by comparison of VSCF-PT2 calculations with cold ion spectroscopy. *Physical Chemistry Chemical Physics.* 2018, 20(38): 24894–24901. doi: 10.1039/c8cp03989e
26. Mollaamin F. Computational Methods in the Drug Delivery of Carbon Nanocarriers onto Several Compounds in Sarraceniaceae Medicinal Plant as Monkeypox Therapy. *Computation* 2023, 11: 84, doi:10.3390/computation11040084
27. Kawczak P, Bober L, Bączek T. QSAR Analysis of Selected Antimicrobial Structures Belonging to Nitro-derivatives of Heterocyclic Compounds. *Letters in Drug Design & Discovery.* 2020, 17(2): 214–225. doi: 10.2174/1570180815666181004112947
28. McArdle S, Mayorov A, Shan X, et al. Digital quantum simulation of molecular vibrations. *Chemical Science.* 2019, 10(22): 5725–5735. doi: 10.1039/c9sc01313j
29. Shahriari S, Monajjemi M, Mollaamin F. Determination of proteins specification with sars- covid-19 based ligand designing. *Journal of the Chilean Chemical Society.* 2022, 67(2): 5468–5476. doi: 10.4067/s0717-97072022000205468
30. Monajjemi M, Mollaamin F, Shojaei S. An overview on coronaviruses family from past to COVID-19: Introduce some inhibitors as antiviruses from Gillan’s plants. *Biointerface Research in Applied Chemistry.* 2020; 3: 5575–5585. doi:10.33263/BRIAC103.575585.
31. Mollaamin F, Ilkhani A, Sakhaei N, et al. Thermodynamic and Solvent Effect on Dynamic Structures of Nano Bilayer-Cell Membrane: Hydrogen Bonding Study. *Journal of Computational and Theoretical Nanoscience.* 2015, 12(10): 3148–3154. doi: 10.1166/jctn.2015.4092
32. Monajjemi M, Khaleghian M, Tadayonpour N, et al. The effect of different solvents and temperatures on stability of single-walled carbon nanotube: A QM/MD study. *International Journal of Nanoscience.* 2010, 09(05): 517–529. doi: 10.1142/s0219581x10007071
33. Monajjemi M, Afsharnezhad S, Jaafari MR, et al. Investigation of energy and NMR isotropic shift on the internal rotation Barrier of  $\Theta_4$  dihedral angle of the DLPC: A GIAO study. *Chemistry* 2008, 17(1), 55–69.
34. Wang S. Efficiently Calculating Anharmonic Frequencies of Molecular Vibration by Molecular Dynamics Trajectory Analysis. *ACS Omega.* 2019, 4(5): 9271–9283. doi: 10.1021/acsomega.8b03364
35. Mollaamin F, Shahriari S, Monajjemi M. Monkeypox Disease Treatment by Tecovirimat Adsorbed onto Single-Walled Carbon Nanotube Through Drug Delivery Method. *Journal of the Chilean Chemical Society.* 2023; 68: 5796–5801. doi: 10.4067/S0717-97072023000105781
36. Ni W, Li G, Zhao J, et al. Use of Monte Carlo simulation to evaluate the efficacy of tigecycline and minocycline for the treatment of pneumonia due to carbapenemase-producing *Klebsiella pneumoniae*. *Infectious Diseases.* 2018, 50(7): 507–513. doi: 10.1080/23744235.2018.1423703
37. Andrews CW, Wisowaty J, Davis AO, et al. Molecular modeling, NMR spectroscopy, and conformational analysis of 3',4'-anhydrovinblastine. *Journal of Heterocyclic Chemistry.* 1995, 32(3): 1011–1017. doi: 10.1002/jhet.5570320357
38. HyperChem, version 8.0; Hypercube Inc: Gainesville, FL, USA (2007).
39. Sarasia EM, Afsharnezhad S, Honarparvar B, et al. Theoretical study of solvent effect on NMR shielding tensors of luciferin derivatives. *Physics and Chemistry of Liquids.* 2011, 49(5): 561–571. doi: 10.1080/00319101003698992
40. Mollaamin F, Shahriari S, Monajjemi M. Drug design of medicinal plants as a treatment of omicron variant (COVID-19 variant B.1.1.529), *Journal of the Chilean Chemical Society.* 2022, 67(3): 5562–5570. doi: 10.4067/s0717-97072022000305562
41. Mollaamin F. Physicochemical investigation of anti-covid19 drugs using several medicinal plants. *Journal of the Chilean Chemical Society.* 2022, 67(2): 5537–5546. doi: 10.4067/s0717-97072022000205537
42. Khaleghian M, Zahmatkesh M, Mollaamin F, et al. Investigation of Solvent Effects on Armchair Single-Walled Carbon Nanotubes: A QM/MD Study. *Fullerenes, Nanotubes and Carbon Nanostructures.* 2011, 19(4): 251–261. doi: 10.1080/15363831003721757
43. Tahan A, Mollaamin F, Monajjemi M. Thermochemistry and NBO analysis of peptide bond: Investigation of basis sets and binding energy. *Russian Journal of Physical Chemistry A.* 2009, 83(4): 587–597. doi: 10.1134/s003602440904013x

44. Shahriari S, Monajjemi M, Zare K. Penetrating to cell membrane bacteria by the efficiency of various antibiotics (clindamycin, metronidazole, azithromycin, sulfamethoxazole, baxdela, ticarcillin, and clavulanic acid) using S-NICS theory. *Biointerface Res. Appl. Chem.* 2018, 8: 3219 -3223.
45. Aihara J. Reduced HOMO–LUMO Gap as an Index of Kinetic Stability for Polycyclic Aromatic Hydrocarbons. *The Journal of Physical Chemistry A.* 1999, 103(37): 7487–7495. doi: 10.1021/jp990092i
46. Kohn W, Becke AD, Parr RG. Density Functional Theory of Electronic Structure. *The Journal of Physical Chemistry.* 1996, 100(31): 12974–12980. doi: 10.1021/jp960669l
47. Parr RG, Pearson RG. Absolute hardness: companion parameter to absolute electronegativity. *Journal of the American Chemical Society.* 1983, 105(26): 7512–7516. doi: 10.1021/ja00364a005
48. Politzer P, Abu-Awwad F. A comparative analysis of Hartree-Fock and Kohn-Sham orbital energies. *Theoretical Chemistry Accounts: Theory, Computation, and Modeling (Theoretica Chimica Acta).* 1998, 99(2): 83–87. doi: 10.1007/s002140050307
49. Silverstein RM, Bassler GC, Morrill TC. *Spectrometric Identification of Organic Compounds*, 5th ed., John Wiley & Sons, Inc., New York, 1981.